Intrinsic dynamics of weakly and strongly confined excitons in nonpolar nitride-based heterostructures

P. Corfdir,[1] J. Levrat,[1] A. Dussaigne,[1] P. Lefebvre,[2,*] H. Teisseyre,[3,4] I. Grzegory,[4] T. Suski,[4] J.-D. Ganière,[1] N. Grandjean,[1] and B. Deveaud-Plédran[1]

[1]*Institute of Condensed Matter Physics, Ecole polytechnique fédérale de Lausanne (EPFL), CH-1015 Lausanne, Switzerland*
[2]*Instituto de Sistemas Optoelectrónicos y Microtecnología, ETSI Telecomunicación, Universidad Politécnica, 28040 Madrid, Spain*
[3]*Institute of Physics, Polish Academy of Sciences, 02-668 Warsaw, Poland*
[4]*Institute of High Pressure Physics, Polish Academy of Sciences, 01-142 Warsaw, Poland*
(Received 28 January 2011; published 30 June 2011)

Both weakly and strongly confined excitons are studied by time-resolved photoluminescence in a nonpolar nitride-based heterostructure grown by molecular beam epitaxy on the *a*-facet of a bulk GaN crystal, with an ultralow dislocation density of 2×10^5 cm^{-2}. Strong confinement is obtained in a 4 nm thick Al$_{0.06}$Ga$_{0.94}$N/GaN quantum well (QW), whereas weakly confined exciton-polaritons are observed in a 200 nm thick GaN epilayer. Thanks to the low dislocation density, the effective lifetime of strongly confined excitons increases between 10 and 150 K, proving the domination of radiative recombination processes. Above 150 K the QW emission lifetime diminishes, whereas the decay time of excitons in the barriers increases, until both barrier and QW exciton populations become fully thermalized at 300 K. We conclude that the radiative efficiency of our GaN QW at 300 K is limited by nonradiative recombinations in the barriers. The increase of exciton-polariton coherence lengths caused by low dislocation densities allows us to observe and model the quantized emission modes in the 200 nm nonpolar GaN layer. Finally, the low-temperature phonon-assisted relaxation mechanisms of such center-of-mass quantized exciton-polaritons are described.

I. INTRODUCTION

Since Waltereit *et al*. demonstrated the realization of polarization-free (Al,Ga)N/GaN quantum wells (QWs) ten years ago, many studies have been carried out on nonpolar GaN and nitride-based heterostructures.[1] Contrary to *c*-plane heterostructures, the absence of built-in electric fields in nonpolar layers allows for the growth of thick QWs while keeping a maximal overlap between electron and hole wave functions. The growth of wide QWs is indeed a key issue to produce high-power nitride-based optoelectronic devices (mainly light-emitting diodes), as they allow reduction of the carrier density in the QW, hence lessening the efficiency of Auger-like mechanisms.[2] However, lattice-mismatched substrates such as sapphire or LiAlO$_2$ are generally used to grow nonpolar GaN, inducing strain in the heteroepitaxial layers.[3,4] Strain relaxation through the generation of dislocations or basal stacking faults leads to a drastic reduction of exciton lifetime: even when sophisticated processing techniques such as epitaxial lateral overgrowth are used, exciton dynamics is dominated by the capture on these extended defects.[5-7]

In the present work, we overcome such difficulties by using molecular beam epitaxy (MBE) to grow a nonpolar nitride-based heterostructure on the *a*-facet of a GaN single crystal elaborated by the combination of a high-pressure solution method and hydride vapor phase epitaxy (HVPE). The present heterostructure consists of a 200 nm GaN epilayer on top of which an Al$_{0.06}$Ga$_{0.94}$N/GaN QW is deposited. We first estimate by cathodoluminescence (CL) the threading dislocation density in the QW to 2×10^5 cm^{-2}. Thanks to such a low density of nonradiative recombination centers, we are able to observe directly by time-resolved photoluminescence (TRPL) the increase of QW radiative lifetime with

temperature (T) through the increase in effective lifetime. We thus demonstrate that even in the absence of a strong exciton localization mechanism comparable to those occurring in (In,Ga)N/GaN QWs, radiative mechanisms dominate the recombination processes in our sample for T up to 150 K. At higher T, we observe a drop in the QW PL lifetime that we relate to the thermal escape of QW excitons toward the (Al,Ga)N barriers and to their subsequent nonradiative recombination in the disordered alloy. In parallel, we show that a dislocation density as low as 2×10^5 cm^{-2} drastically reduces exciton scattering events, making possible the observation of exciton-polariton center-of-mass quantization (CMQ) in nonpolar GaN. This observation is supported by a model accounting for the quantization of exciton-polariton center-of-mass motion in the 200 nm thick GaN epilayer. Finally, we describe qualitatively the relaxation mechanisms of these exciton-polaritons at 10 K.

II. EXPERIMENTAL DETAILS

In order to obtain our (11-20) oriented substrates (nonpolar), we used a two-stage growth process. Thin hexagonal platelet crystals were grown by the high-pressure solution method[8,9] from liquid gallium at a nitrogen gas pressure on the order of 1.0 GPa. The important advantage of this method is that the resulting GaN crystals are almost free of structural defects (not exceeding 10^2 cm^{-2}). These hexagonal platelets were used afterward as seeds for HVPE growth. Due to the relatively high crystallization rates (100 μm/h) which may be obtained by HVPE, we are able to grow crystals about a few millimeters thick and with a dislocation density on the order of 5×10^5 cm^{-2}. The single crystal is then oriented and cut by a wire saw along the (11-20) planes. Finally, the substrate is

polished in two stages, first with dry diamond powder and then mechano-chemically before film deposition. The x-ray rocking curve full width at half maximum for the (110) reflection for an illuminated area of 0.8 mm × 1 mm is 27 arcsec, testifying to the low dislocation density of the GaN substrate.[10]

The heterostructure was then grown by MBE on top of the (11-20) facet of the GaN crystal. We set the growth temperature and growth rate to 800 °C and 1 monolayer/s, respectively. The nitrogen source was provided by pyrolytic decomposition of ammonia at the sample surface. We first grew a 200 nm thick GaN layer on the nonpolar GaN crystal. Whereas the GaN substrate is slightly n-doped (free electron concentration n of about 5×10^{17} cm^{-3}), the layer grown by MBE is unintentionally n-doped ($n = 5 \times 10^{16}$ cm^{-3}). Therefore, the n-n^+ interface between the homoepitaxial layer and the substrate prevents holes and thus excitons from leaving the GaN homoepitaxial layer. The doping difference between the substrate and the epilayer also leads to a slight change in refractive index between the two layers.[11] We then deposited on top of the structure a 160 nm Al$_{0.06}$Ga$_{0.94}$N layer, followed by a single 4 nm thick GaN QW that we capped with a 30 nm thick Al$_{0.06}$Ga$_{0.94}$N barrier. Note that we used NH$_3$-MBE rather than plasma-assisted MBE (PAMBE), as the latter technique induces bilayer well-width fluctuation[12] The subsequent stronger exciton localization for PAMBE-grown QWs would have been detrimental to our study of QW free exciton dynamics with temperature.

CL was measured at 300 K using a probe current of 3 nA and an acceleration voltage of 3 kV in order for the carriers to be generated exclusively in the QW and in the (Al,Ga)N barriers. The spatial extension of the generation volume was estimated from the analytical models described in Refs. 13 and 14. The CL signal was collected by a parabolic mirror and sent to a monochromator, followed by a cooled charge-coupled device (CCD). Time-integrated and TRPL experiments were carried out with the third harmonic ($\lambda = 280$ nm) of a Ti: Al$_2$O$_3$ mode-locked laser (pulse width and repetition rate of 2 ps and 80.7 MHz, respectively). The laser beam was focused down to a 40 μm spot on the sample surface. We estimate that the photogenerated carrier density was about 5×10^{10} cm^{-2} in the QW. The PL was analyzed with a 1200 grooves/mm grating followed by a streak camera working in synchroscan mode. Continuous-wave PL was carried out at 4 K with the 244 nm line of a frequency-doubled argon laser and a 2400 grooves/mm grating. Finally, excitation-dependent PL spectra have been obtained with a quasi-continuous-wave Nd : YAG (yttrium-aluminum-garnet) laser.

III. ROOM-TEMPERATURE CATHODOLUMINESCENCE

Room-temperature CL mapping of Al$_{0.06}$Ga$_{0.94}$N/GaN QW taken at the QW emission energy is shown in Fig. 1. The black spots observed on the CL mapping correspond to nonradiative recombination centers, which we ascribe to the emergence of threading dislocations.[15] From the CL map, we deduce a dislocation density of 2×10^5 cm^{-2}, a density approximately four orders of magnitude smaller than the dislocation densities reported for nonpolar GaN grown on sapphire.[16,17] Contrary to what is observed for structures grown on lattice-mismatched substrates, the absence in the
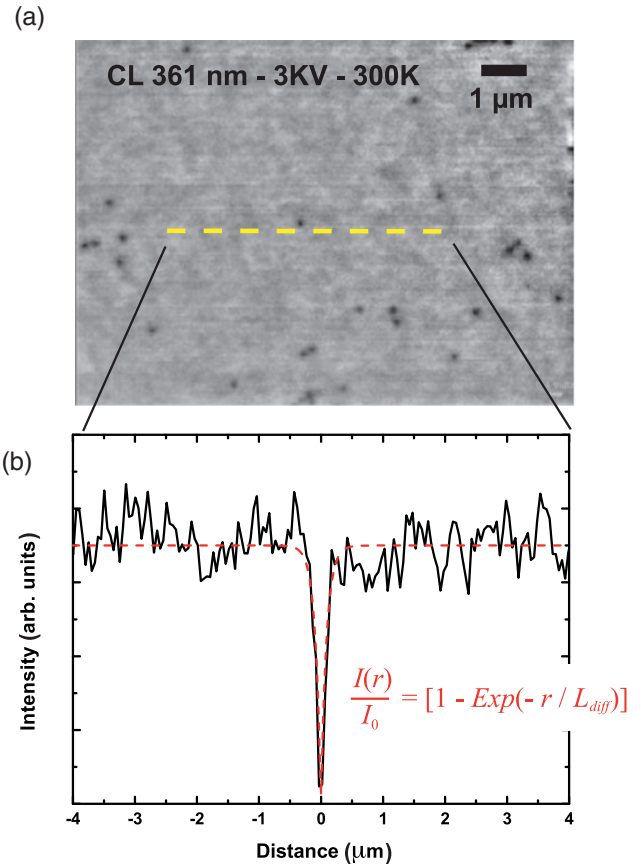

FIG. 1. (Color online) (a) Room-temperature top-view cathodoluminescence mapping of Al$_{0.06}$Ga$_{0.94}$N/GaN QW taken at the QW emission energy. We attribute the black spots to the emergence of threading dislocations and we deduce a dislocation density of 2×10^5 cm^{-2}. (b) The analysis of the CL intensity in the vicinity of a dislocation (yellow dashed line) yields an exciton diffusion length $L_{\mathrm{diff}} = 100$ nm at 300 K.

CL mapping of striped contrasts parallel to the c- or the m-axes evidences that our sample is free of basal plane and prismatic stacking faults.[18] Finally, from the analysis of the CL intensity in the vicinity of a dislocation,[19] we deduce that the diffusion length L_{diff} of QW excitons is below 100 nm at 300 K. Therefore, in a PL experiment, only a small fraction of photogenerated excitons is affected by dislocations at room temperature.

IV. TIME-INTEGRATED AND TIME-RESOLVED PHOTOLUMINESCENCE WITH TEMPERATURE

The time-integrated PL at low temperature is shown in Fig. 2(a). At 10 K, the QW emission is centered at 3.494 eV (full width at half maximum of 11 meV), while the emission at 3.58 eV is assigned to the (Al,Ga)N barriers. The luminescence at 3.471 eV is attributed to the recombination of donor-bound excitons ($D^\circ X$) in the GaN buffer.[20] The latter is excited by the QW emission rather than directly by the laser, as the laser light is principally absorbed within the first ~100 nm at the sample surface.[21] As will be discussed later on, the transitions between 3.474 and 3.486 eV [Fig. 2(b)] are the signatures of the quantization of exciton-polariton
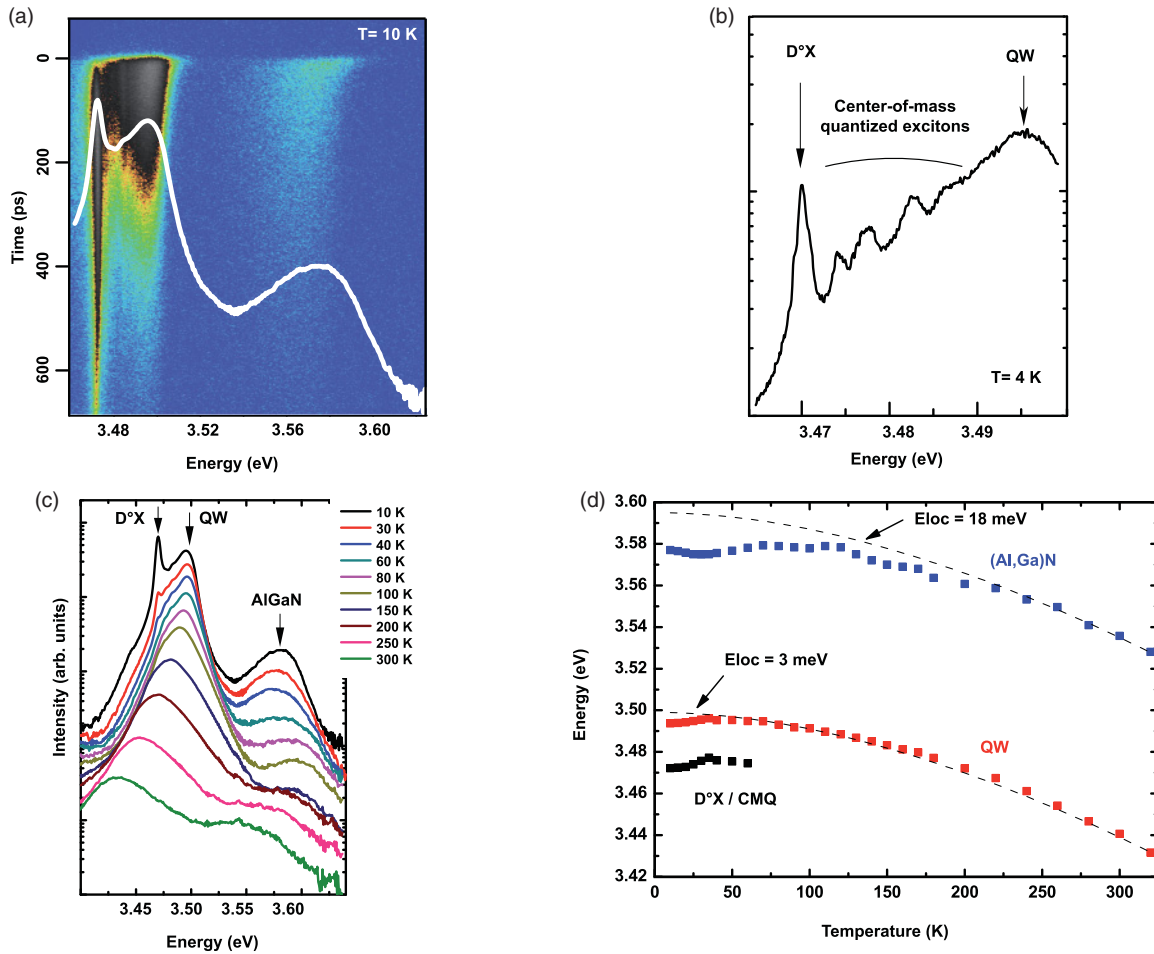
FIG. 2. (Color online) (a) Time-resolved PL image of the 4 nm thick $Al_{0.06}Ga_{0.94}N$/GaN QW at 10 K. (b) cw-PL spectrum taken at 4 K, showing the signature of center-of-mass quantized exciton-polaritons in the 200 nm thick GaN layer. (c) Time-integrated PL spectra taken between 10 and 300 K (spectra have been shifted vertically for clarity). The absence of emission at 3.42 eV shows that our sample is free of basal plane stacking faults. At 10 K, the full width at half maximum of the QW emission is 11 meV. Above 200 K, the QW and (Al,Ga)N emissions exhibit the same high-energy slopes, indicating that both exciton populations are thermalized. (d) QW, (Al,Ga)N barriers, and $D°X$/center-of-mass quantized (CMQ) emission energies with temperature (red, blue, and black symbols, respectively). Dashed lines are Varshni fits of the QW and (Al,Ga)N emission energies evolutions with temperature. The 3 meV blueshift of the QW emission between 10 and 30 K is attributed to the delocalization of QW excitons toward the two-dimensional continuum of states.

center-of-mass motion along the growth axis in the 200 nm GaN epilayer. When increasing T from 10 to 30 K the QW emission is slightly blueshifted [Fig. 2(d)]. Such a half S-shaped T dependency of the QW emission energy is characteristic of the delocalization of excitons toward the continuum of two-dimensional states of the QW.[22,23] From the difference between the QW emission energy at 10 K and the extrapolation at 0 K of the high-T dependence of QW emission energy, we deduce a QW exciton localization energy $E_{loc} = 3 \pm 1$ meV [Fig. 2(d)]. As a comparison, we recently reported a localization energy of 9 meV for excitons confined in a 4 nm thick a-plane $Al_{0.05}Ga_{0.95}N$/GaN QW grown on epitaxial laterally overgrown (ELO) GaN,[24] indicating that the use of bulk GaN crystal certainly allows for more homogeneous Al-atom incorporation in the barrier and for a better control of the QW thickness. Note also that the localization energy deduced for the present QW agrees well with the 3.5 meV localization energy that we calculate by envelope function calculations[25] for an exciton bound to a

single monolayer well-width fluctuation. At higher T, the QW emission energy redshifts and its evolution with T follows that of the GaN band gap.

The temperature dependence of (Al,Ga)N barriers emission energy exhibits a full S-shaped behavior, an indication of exciton localization inside this disordered alloy [Fig. 2(d)]. Between 10 and 30 K, the (Al,Ga)N emission redshifts, which we attribute to the ionization of excitons bound to the shallower potential fluctuations in favor of the deeper ones. Concerning the blueshift part of the S-shape, it is related to the delocalization of excitons toward the three-dimensional continuum of states of the barriers. From the extrapolation at 0 K of the temperature dependence of (Al,Ga)N free exciton energy, we extract an exciton localization energy of 18 meV in the barriers. We attribute these rather large fluctuations in barrier Al composition to the anisotropic incorporation of Al atoms when growing along nonpolar planes. Note that this 18 meV localization for excitons in the (Al,Ga)N barriers agrees with the time dependence of the low-temperature
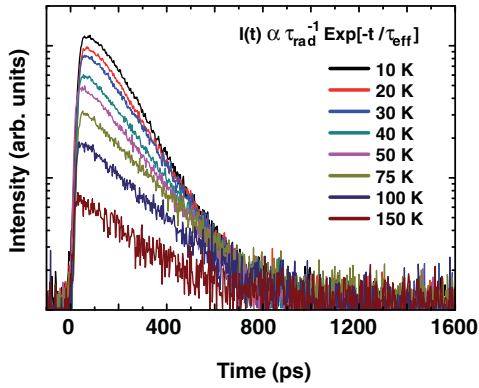
FIG. 3. (Color online) QW PL transients between 10 and 150 K. The QW emission intensity at zero delay is inversely proportional to the radiative lifetime $\tau_{\rm rad}$. The PL decay time $\tau_{\rm eff}$ is given by $\tau_{\rm eff}^{-1} = \tau_{\rm rad}^{-1} + \tau_{\rm nrad}^{-1}$, where $\tau_{\rm nrad}$ is the QW nonradiative lifetime. The reduction in PL intensity at zero delay combined with the increase in lifetime with temperature evidences the expected increase of radiative lifetime with T and the minor role played by nonradiative recombinations in that temperature range.

(Al,Ga)N PL spectrum, which exhibits a large redshift during the first 100 ps of decay [Fig. 2(a)]. From these variations in the (Al,Ga)N energy band gap, combined with our envelope function calculations,[25] we deduce that such a barrier disorder should induce a ± 1 meV variation of QW exciton emission energy.

The dynamical behavior of the QW PL is shown in Fig. 3. At 10 K, excitons are localized and decay radiatively with a decay time of $\tau_{\rm loc} = 110$ ps. This radiative lifetime is 2–4 times shorter than what has been reported so far for nonpolar (Al,Ga)N/GaN QWs of the same thickness grown on Al_2O_3 or $LiAlO_2$.[1,5,24,26] Similarly to what occurs for excitons bound to impurities in bulk semiconductors,[27] the radiative decay rate of QW localized excitons increases when the coherence volume of the exciton increases.[28] Although not intuitive but experimentally observed,[29] this implies that the larger the spatial extension of localized states in a QW, the shorter the localized exciton lifetime. Consequently, localized state spatial extension in our sample is 2–4 times larger than that of QWs of similar thickness presented in Refs. 1, 5, 24, and 26. We underline that the expected large in-plane spatial extension of QW localization centers in our sample is strongly supported by the relatively small QW exciton localization energy of 3 meV deduced above, as compared to our previous results on QWs grown on ELO-GaN.[24]

When increasing T, the effective PL decay time $\tau_{\rm eff}$ averaged spectrally over the contributions of both localized and free excitons first increases from 110 ps at 10 K up to 350 ps at 150 K (Fig. 3) and then steadily decreases for higher T [Fig. 4(b)]. In parallel, the initial PL intensity $I(t=0)$ continuously decreases between 10 and 320 K. As above 10 K, the thermal escape of QW bound excitons toward the whole two-dimensional continuum of states is activated Fig. 2(d)]; the increase of $\tau_{\rm eff}$ combined with the decrease of $I(t=0)$ indicates that the average radiative decay time of free and localized excitons increases with T. Although the direct observation of longer radiative lifetime through the increase in effective lifetime is now common in III-arsenides or II-VI

QWs,[30] it has, to our knowledge, only been reported once in polar (Al,Ga)N/GaN multiple QWs for T between 10 and 60 K.[31] In most polar and nonpolar nitride-based QWs, even when processed by epitaxial lateral overgrowth,[5] nonradiative processes are dominant and mask the intrinsic increase of QW exciton radiative lifetime with T.[32] Deconvolution of the experimental decay between radiative and nonradiative contributions as well as guesses on the QW low-T radiative efficiency then must be done to estimate exciton radiative lifetime, a procedure resulting in radiative lifetimes determined with a low accuracy. Here, the entire suppression of electric fields and the reduction of dislocation density allow on the contrary for the direct measurement of the QW radiative lifetime increase with T. Note finally that the T-dependence of the radiative efficiency of our low Al-content barrier (Al,Ga)N/GaN QW cannot be straightforwardly compared with that of (In,Ga)N-based QWs. In (In,Ga)N/GaN QWs, excitons are indeed strongly localized along the QW plane and are therefore likely preserved even at 300 K from reaching nonradiative recombination centers.[33] This is absolutely not the case here as we measure that QW excitons are already delocalized at 30 K (Fig. 2).

V. THEORETICAL MODEL AND FITTING PROCEDURE

Accounting for both the delocalization of bound excitons[28] and the thermal distribution of free excitons in k-space,[32] and assuming that the populations of free and bound excitons are in thermal equilibrium at all times (relaxation processes are much faster than recombinations as the energy separation between these states is small), the average decay rate for QW excitons is

$$\Gamma = (N_{\rm loc}\Gamma_{\rm loc} + N_{\rm fr}\Gamma_{\rm fr})/(N_{\rm loc} + N_{\rm fr}) = 1/\tau_{\rm eff}, \quad (1)$$

where $N_{\rm loc}$ and $N_{\rm fr}$ are the respective densities of localized and free excitons and $N = N_{\rm loc} + N_{\rm fr} = 5 \times 10^{10}$ cm^{-2} is the total density of photogenerated excitons. Under nondegenerate excitation conditions, excitons follow Boltzmann distributions:

$$N_{\rm fr}(T) \approx \frac{2MkT}{\pi\hbar^2}\exp\left(-\frac{E_X(T) - E_F}{kT}\right) \quad (2)$$

and

$$N_{\rm loc}(T) \approx N_D\exp\left(-\frac{E_X(T) - E_{\rm loc} - E_F}{kT}\right), \quad (3)$$

with $M = m_e + {\rm m}_h = 1.2\,m_0$ is the exciton mass,[34] N_D is the areal density of localization centers in the QW, $E_X(T)$ is free exciton A recombination energy, and $E_{\rm loc} = 3$ meV is the localization energy of QW excitons obtained from Fig. 2(d). The Fermi level energy for excitons is then given by

$$E_F(T) = E_X(T) + kT\ln\frac{N}{2\frac{MkT}{\pi\hbar^2} + N_D\exp\left(\frac{E_{\rm loc}}{kT}\right)}. \quad (4)$$

Exciton densities $N_{\rm fr}$ and $N_{\rm loc}$ can thus be expressed as a function of a single unknown parameter N_D. While the decay rate of localized excitons $\Gamma_{\rm loc} = \tau_{\rm loc}^{-1}$ is independent of T, the free exciton decay rate is $\Gamma_{\rm fr}(T) = \Gamma_{\rm r}(T) + \Gamma_{\rm nr}(T)$, with $\Gamma_{\rm r}$ and $\Gamma_{\rm nr}$ the free exciton radiative and nonradiative decay rates,

respectively. As a result of the thermal population of states lying out of the light cone, Γ_r decreases linearly with T,[32]

$$\tau_r(T) = \frac{1}{\Gamma_r(T)} = \frac{6Mk_BT}{\hbar^2 k_0^2 \Gamma_0}, \qquad (5)$$

where k_0 is the in-plane wave vector above which the decay rate of the QW free exciton is zero. At $k_{//} = 0$, the decay rate of longitudinal and transverse free excitons $\Gamma_0 = e^2 f_{osc}/(4m_0 \varepsilon_0 cnS)$ is proportional to the exciton oscillator strength per unit area f_{osc}/S (n is the optical index of GaN and the other constants have their usual meanings).[32] The corresponding radiative lifetime of 2.4 ps for free excitons at $k_{//} = 0$ has been determined previously by TRPL on thin polar (Al,Ga)N/GaN QWs.[35] Such a short radiative lifetime compared to the 10 ps measured in (Al,Ga)As/GaAs QWs (Ref. [36]) arises simply from the longitudinal-transverse splitting that is larger by a factor of 6 in GaN than in GaAs.[37] In order to understand the decrease of τ_{eff} for T higher than 150 K, we consider a thermally activated nonradiative recombination process with activation energy E_a:

$$\tau_{nr}(T) = \Gamma_{nr}(T)^{-1} = \tau_1 \exp(-E_a/kT). \qquad (6)$$

The experimental evolution of τ_{eff} versus T is accounted for by adjusting three parameters: while E_a and τ_1 play a significant role only above 150 K, the only parameter fitting the low-T dependence of τ_{eff} is N_D. Accounting for the ± 1 meV experimental uncertainty on the determination of E_{loc}, we find $N_D = 3.0 \pm 0.5 \times 10^{12}$ cm (Fig. 4). Such a high density might be surprising compared with the best (Al,Ga)As/GaAs QWs, where exciton localization occurs on flat islands resulting from steplike monolayer variations of the well width, with typical densities between 10^{10} and 10^{11} cm^{-2}.[38] The estimation

of localization centers density is however more complex in (Al,Ga)N/GaN QWs. First, the growth is step-flow and the growth rates are different for the in-plane c- and m-axes.[39] Moreover, the large effective mass of holes in GaN makes excitons quite sensitive to the statistical distribution of Al atoms in the barriers, allowing for localization even in the absence of well width fluctuation or segregation in the ternary alloy.[40] Finally, we note that the interatomic distances in GaN are smaller than those in GaAs. The areal atomic density in III-nitrides is therefore approximately a factor of 2 higher than in III-arsenides. From this steric argument, we conclude that the areal density of localization centers in GaN QWs must be higher than that in GaAs QWs.

Regarding the high-T evolution of τ_{eff}, we find $\tau_1 = 50 \pm 16$ ps and $E_a = 43 \pm 7$ meV. We first rule out that nonradiative recombinations may arise from the capture of excitons by dislocations: as shown in Fig. 1, at 300 K, only excitons generated less than 100 nm away from a dislocation can diffuse to it and recombine nonradiatively. We rather infer that excitons thermally escape the QW toward the (Al,Ga)N barriers.[30] In the high-T regime, both QW and barriers exciton populations are indeed thermalized [Fig. 2(c)], and τ_{eff} is given by the average between barriers and QW decay times, weighted by the respective effective density of states. As shown in Fig. 4(b), τ_{eff} is clearly limited by the lifetime of excitons of the disordered (Al,Ga)N barriers, even if we cannot discern if the latter is controlled by nonradiative recombination on point defects or by surface recombination. Nevertheless, our result demonstrates that the use of bulk GaN substrates has allowed us to achieve light emitters whose efficiency is limited by the thermal escape of charge carriers from the QW to the barriers. The latter phenomenon should thus be tackled
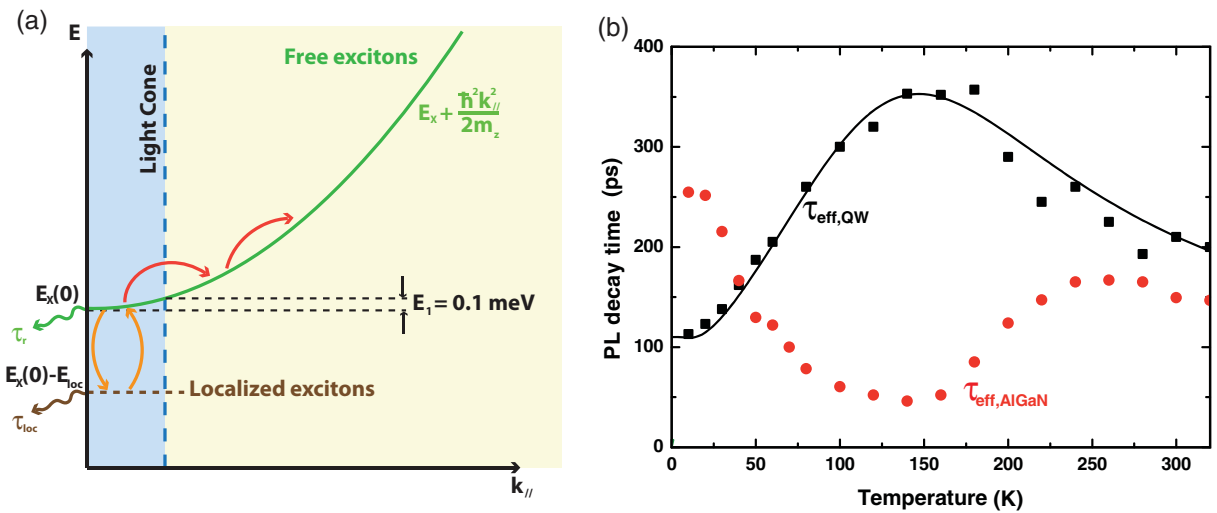

FIG. 4. (Color online) (a) Dispersion curves for free and bound QW excitons. Thanks to fast relaxation processes compared with recombination mechanisms, localized and free exciton populations N_{loc} and N_{fr} are in thermal equilibrium. In parallel, free excitons are thermally distributed in k-space and excitons with kinetic energy larger than 0.1 meV lie out of the light cone. For a given excitation density, the relative density of dark excitons increases with temperature and the average QW exciton decay rate decreases. (b) Experimental (black squares) and calculated (solid line) QW exciton effective lifetime with temperature. Experimental (Al,Ga)N barriers PL decay time is shown with red circles. Fitting QW exciton decay time evolution in the low-temperature range yields a QW exciton oscillator strength of 5×10^{13} cm^{-2} and a QW localized states density of $3.0 \pm 0.5 \times 10^{12}$ cm^{-2}. Above 150 K, the QW PL effective lifetime decreases due to the thermal escape of QW excitons toward the (Al,Ga)N barriers. In parallel, (Al,Ga)N PL decay time increases, until QW and barriers exciton populations are fully thermalized and exhibit the same PL lifetimes.

by increasing the carrier's confinement, which we propose to obtain by increasing the QW width rather than the barrier Al content in order to keep the emission PL broadening as low as possible.

VI. EXCITON CENTER-OF-MASS QUANTIZATION

The limitations induced by high dislocation densities do not rely solely on their nonradiative character. Whereas its weak spin-orbit coupling promised GaN for spin transport applications over long distances,[41] carrier spin relaxation times are limited to tens of picoseconds due to scattering with dislocations.[42] Similarly, exciton-polariton CMQ, a widely considered optical signature of crystalline perfection and homogeneity of semiconductor thick layers, has been reported in thick CdS and CdSe layers since the early 1970s[43] and for almost twenty years in CdTe[44] and GaAs,[45] whereas it has only been reported once for polar GaN.[11] Such a gap between the optical properties of nitrides and other classes of semiconductors also originates from dislocations that limit exciton coherence length—i.e., the distance covered by an exciton between two dephasing events—and prevents the formation of polariton standing waves along the growth axis. We thus expect from the reduced dislocation density in our sample a significant increase of polariton coherence length, which is evidenced by the four emission lines observed in the low-temperature spectra and lying at 3.474, 3.478, 3.483, and 3.486 eV (with full width at half maximum of 3.0, 3.0, 2.0, and 2.0 meV, respectively) [Fig. 5]. The observation of emission lines with comparable intensities over such a broad energy range (12 meV) is indeed reminiscent of the emission from CMQ exciton-polariton modes. In the GaN epilayer of thickness $L = 200$ nm comprised between the bottom (Al,Ga)N barrier and the n^+ GaN substrate, excitons can be considered confined *as a whole*. The momentum of their center of mass along the growth direction is quantized and only assumes the values that fulfill:[46]

$$\begin{cases} k_n \tan(k_n L/2) + \tanh(L/2a_B)/a_B = 0 ; & n = 1,3,5,... \\ \tan(k_n L/2)/k_n - a_B \tanh(L/2a_B) = 0 ; & n = 2,4,6,... \end{cases}$$
(7)

where k_n is the wave number of exciton center of mass for the nth allowed mode and a_B is the exciton Bohr radius. Additional selection rules can also appear due to the parity of the exciton wave function along the confinement direction, which is not the case for our given photon wave vector and layer thickness L.[44] The wave numbers determined with Eq. (7) correspond to allowed confined mode energies, according to the exciton-polariton dispersion curves of the material. To compute the dielectric function we use the dielectric background constant ε_b and exciton A, B, and C resonances. Transverse excitons of energies E_T and masses M are modeled as damped harmonic oscillators with oscillator strength f_{osc} and damping constant Γ. The polariton dispersion curve $E(k)$ is obtained by equaling the dielectric function to the photon dispersion:[47]

$$\frac{\hbar^2 c^2 k^2}{E} = \varepsilon_b + \sum_{i=1}^{3} \frac{f_{osc} E_{T,i}^2}{E_{T,i}^2 - E^2 + \hbar^2 E_{T,i} k^2/M_i - i\hbar\Gamma_i E}.$$
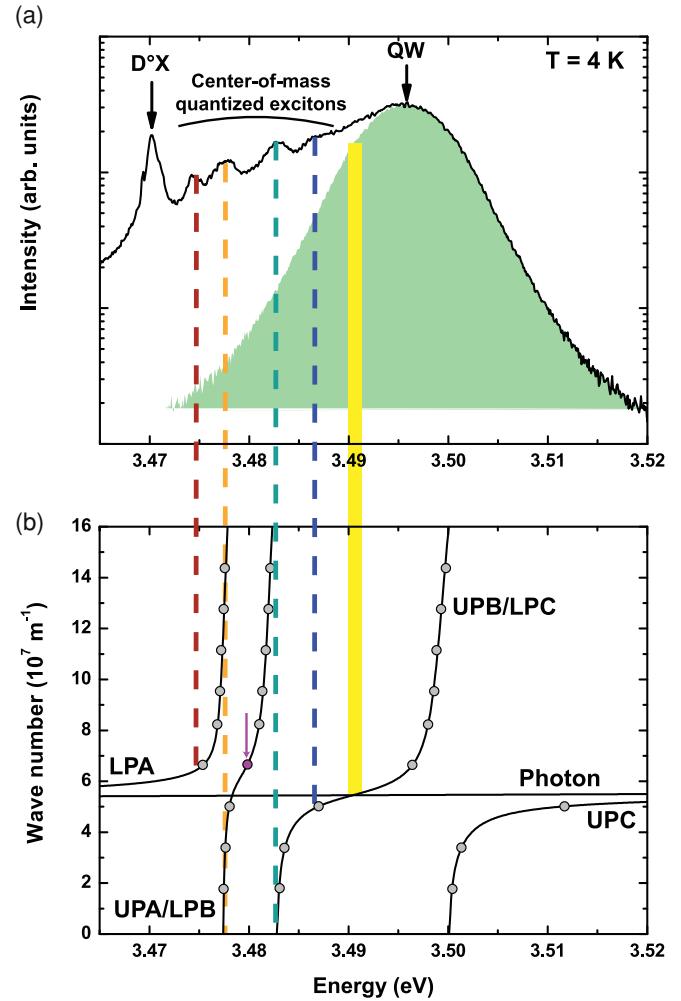(8)

FIG. 5. (Color online) (a) Low-temperature time-integrated PL spectrum. The emission lines at 3.474, 3.478, 3.483, and 3.486 eV are attributed to center-of-mass quantized exciton-polaritons in the 200 nm thick GaN epilayer. (b) Light and polariton dispersion curves (solid lines) and allowed emission modes (circles) in the 200 nm thick GaN epilayer. The emission from the polariton mode at 3.480 eV (magenta dot pointed out by an arrow) is not observed because of its weak photon character. Lower and upper polariton branches are, respectively, denoted by LP and UP. The QW luminescence at 3.492 eV (yellow line in the figure) is resonant with the UPB/LPC polariton branch of the GaN epilayer. Photoexcited polaritons relax through the emission of acoustic phonons toward lower-energy modes, and then decay radiatively, giving rise to the emission at 3.474, 3.478, 3.483, and 3.486 eV, or get trapped by donors to form donor bound excitons emitting at 3.471 eV.

The parameters f_{osc}, Γ, and ε_b are those given in Ref. 48, while we took for E_T the values reported for homoepitaxial GaN in Ref. 20. Figure 5 shows that the emission lines at 3.478 and 3.483 eV result from the superposition of allowed modes on the weakly dispersive parts of the A and B branches. On the contrary, the transitions at 3.474 and 3.486 eV are related to single confined photonlike modes located on strongly dispersive parts of the dispersion curves. Although there is so far a good agreement between the computed values and the experimental spectra, an emission mode expected at 3.480 eV is not observed [magenta dot pointed out by an arrow in
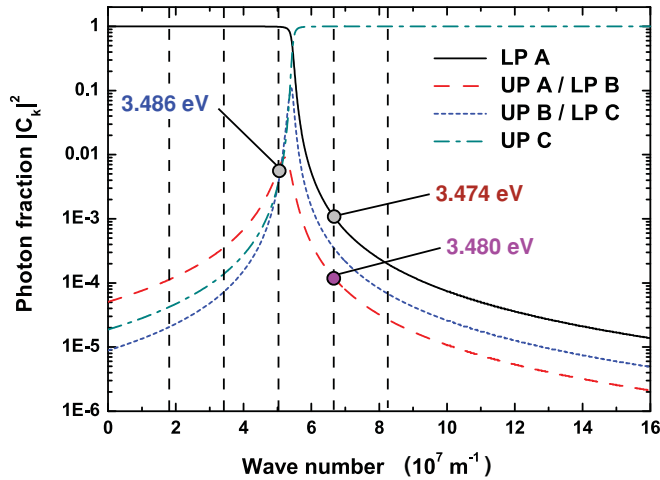
FIG. 6. (Color online) Calculated photon fraction with respect to the wave vector for LPA, UPA/LPB, UPB/LPC, and UPC polariton branches (black solid line, red dashed line, blue dotted line, and cyan dash-dotted line, respectively). Dashed vertical lines show the quantized wave vectors in the 200 nm thick GaN epilayer. The gray dots show the single exciton-polariton modes giving rise to the emission at 3.474 and 3.486 eV. The magenta dot points to the mode at 3.480 eV not observed experimentally because its photon character is too weak.

Fig. 5(b)]. We have consequently applied the quasiparticle model[49] to access for all k to the expansion coefficients of each polariton on a basis built with A-B-C excitons and photon eigenstates (Fig. 6). We took exciton/photon coupling constants of 25, 15, and 15 meV for excitons A, B, and C, respectively.[50] We have not included exciton linewidths in our model since their impact is negligible for broadenings smaller than 25 meV. As shown in Fig. 6, we find first that the mode at 3.486 eV is the one with the strongest photon character, explaining why the PL intensity of this single polariton mode is comparable to the total contribution of the numerous excitonlike modes lying at 3.478 and 3.483 eV. Moreover, the single mode at 3.480 eV exhibits a photon fraction one order of magnitude smaller than the modes at 3.486 and 3.478 eV: the exciton-light coupling is therefore poor for this mode that consequently appears dark in Fig. 5(a).

We emphasize that given their energy separation from the QW emission, we can safely discard the possibility that the lines between 3.474 and 3.486 eV would originate from monolayer fluctuations of the QW width.[22,23] Increasing the excitation density indeed does not lead to any saturation of these lines, as would be the case for QW localized states (Fig. 7). When moving the excitation spot on the surface of the sample, neither an energy shift nor a change in the relative intensities of these transitions is observed. Despite the fact that similar lines have already been seen in high-quality c-plane GaN layers[20,51] and that the emissions at 3.478 and 3.483 eV correspond to the recombination energies of the A and B free exciton ground state in strain-free GaN, respectively, the emissions from A and B exciton excited states as well as that from the free exciton C ground state lie at too high an energy to be related to the 3.486 eV transition.[20] We exclude as well $D°X$ rotator states as the possible origin of the emission at
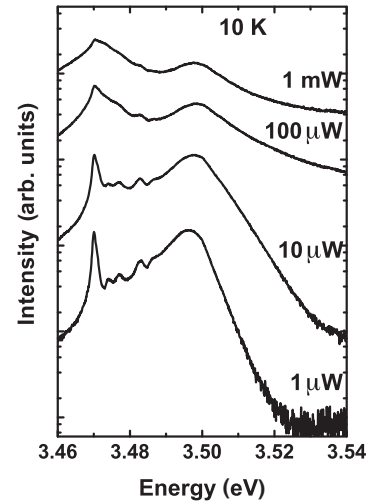

FIG. 7. Quasi-continuous-wave PL at 10 K carried out with a pulsed Nd : YAG laser. Increasing the excitation density does not lead to any saturation of the emission lines at 3.474, 3.478, 3.483, and 3.486 eV. On the contrary, increasing the excitation density from 1 μW to 1 mW increases the density of upper-B/lower-C polaritons excited by the QW PL.

3.474 eV for several reasons. The intensity ratio[51] as well as the energy separation between the $D°X$ ground and excited states[52] only depend on the internal structure of the $D°X$ and do not match at all with the lines observed here (Fig. 2). We also do not detect at 3.45 eV the sharp emissions from the $D°X$ two-electron replica that always accompany the observation of $D°X$ rotator states (Fig. 2). In addition, we emphasize that while an increase in temperature leads as expected to a fast quenching of the $D°X$ (Ref. 53) [Fig. 2(c)], it is not the case for the lines between 3.474 and 3.486 eV. The latter behavior is an additional indication of the intrinsic origin of the 3.474 to 3.486 eV lines. If these lines were related to bound excitons, we would have on the contrary observed a faster quenching of the PL for these high-energy lines as these bound excitons would have been ionized more easily. The observation of CMQ exciton-polaritons is consequently attested, evidencing that the exciton coherence length along the a-axis largely exceeds 400 nm in our nonpolar homoepitaxial GaN epilayer. Finally, while in-plane disorder at the exciton-scale (e.g., monolayer width fluctuation) results in variation of the quantized wave numbers and in a broadening of the center-of-mass quantized exciton-polariton emission modes, the in-plane distribution of dislocations is much more critical. As the lateral in-plane extension of a polariton is given by the photon wavelength, the minimal in-plane separation between two dislocations must indeed be a few hundred nanometers in order for exciton-polariton standing waves to form. As the dislocation density in our sample is 2×10^5 cm^{-2} (Fig. 1), we therefore *a posteriori* verify that the scale of the in-plane disorder is large enough to make possible the observation of center-of-mass quantized exciton-polaritons.

Regarding the relaxation of center-of-mass quantized exciton-polaritons, the system is clearly far from thermal equilibrium. If the whole population of center-of-mass quantized excitons followed a Boltzmann distribution, one would

simply expect the emission from the polariton modes at 3.483 and 3.486 eV to be totally quenched at 10 K, whatever their photon weight. As we observe the PL from nonthermal polariton states over a 12 meV range, the relaxation of center-of-mass quantized polaritons is not efficient. In the low-excitation regime, exciton relaxation from high to low *k*-states occurs mainly through the emission of acoustic phonon. The inefficiency of the latter mechanism results in a relaxation bottleneck for excitons. This is due to the low density of exciton states available at low wave vectors and to the reduction of the exciton/acoustic phonon scattering rate for high phonon wave vectors.[54] It should be noted that compared with an infinite crystal, the absence of dispersion along the confinement axis for excitons in our 200 nm thick GaN layer further hinders acoustic-phonon-assisted relaxation due to additional reduction in the density of available final states.

When increasing the excitation density (Fig. 7), exciton relaxation is facilitated due to exciton elastic scattering with other excitons, electrons or holes. In our specific case, the upper B/lower C polariton branch is resonantly excited by the QW PL and we only have to deal with exciton-exciton scattering. Under high excitation densities, scattering between center-of-mass quantized excitons extends their distribution in *k*-space until scattered excitons gain enough energy to relax through the emission of an LO phonon. As the latter mechanism is much more efficient than relaxation through the emission of acoustic phonons,[55] the whole population of center-of-mass quantized excitons relaxes more efficiently. Under high excitation conditions, the emission from the fundamental confined state at 3.474 eV is thus promoted compared to the higher-energy modes at 3.478, 3.483, and 3.486 eV.

VII. CONCLUSIONS

In conclusion, we have grown by molecular beam epitaxy an $Al_{0.06}Ga_{0.94}N$/GaN QW directly on the *a*-facet of a bulk GaN crystal. The resulting heterostructure presents a dislocation density on the order of 2×10^5 cm^{-2}, four orders of magnitude lower than what is observed in heterostructure grown on foreign substrates. Our experiments clearly demonstrate that in the 10–150 K temperature range, even when excitons are delocalized in the whole QW plane, radiative mechanisms dominate the recombination processes. At higher temperature, we observe the thermal escape of excitons from the QW toward the (Al,Ga)N barriers and we attribute the drop in QW PL lifetime to nonradiative recombinations in the barriers. We also show that such a low dislocation density considerably reduces scattering events undergone by excitons, making it possible to observe exciton-polariton center-of-mass quantization in nonpolar GaN. From excitation-dependent photoluminescence experiments, we describe the phonon-assisted relaxation of these center-of-mass quantized exciton-polaritons. In particular, we propose that the low scattering rate of center-of-mass quantized exciton-polaritons with acoustic phonons arises from their absence of dispersion along the growth axis. We believe the outcomes of our study to be of importance. We have indeed demonstrated the realization of nonpolar nitride-based UV emitters with high radiative efficiency at high temperatures and without strong exciton localization mechanisms. More generally, we are confident that the realization of nonpolar nitride-based heterostructures with a low extended defect density paves the way for the extension at room temperature of the physics panorama demonstrated at cryogenic temperature for III-arsenides and II-VI semiconductors.

*Present address: Laboratoire Charles Coulomb UMR 5221 CNRS-UM2, Département Semiconducteurs, Matériaux et Capteurs, Université Montpellier 2, 34095 Montpellier Cedex 5, France.

[1]P. Waltereit, O. Brandt, A. Trampert, H. T. Grahn, J. Menniger, M. Ramsteiner, M. Reiche, and K. H. Ploog, Nature (London) **406**, 865 (2000).

[2]N. F. Gardner, G. O. Müller, Y. C. Shen, G. Chen, S. Watanabe, W. Götz, and M. R. Krames, Appl. Phys. Lett. **91**, 243506 (2007)

[3]B. Imer, F. Wu, S. P. DenBaars, and J. S. Speck, Appl. Phys. Lett. **88**, 061908 (2006).

[4]X. Ni, Ü. Özgür, Y. Fu, N. Biyikli, J. Xie, A. A. Baski, H. Morkoç, and Z. Liliental-Weber, Appl. Phys. Lett. **89**, 262105 (2006)

[5]P. Corfdir, P. Lefebvre, L. Balet, S. Sonderegger, A. Dussaigne, T. Zhu, D. Martin, J.-D. Ganière, N. Grandjean, and B. Deveaud-Plédran, J. Appl. Phys. **107**, 043524 (2010).

[6]M. J. Kappers, J. L. Hollander, C. F. Johnston, C. McAleese, D. V. Sridhara Rao, A. M. Sanchez, C. J. Humphreys, T. J. Badcock, and P. Dawson, J. Cryst. Growth **310**, 4983 (2008).

[7]T. J. Badcock, P. Dawson, M. J. Kappers, C. McAleese, J. L. Hollander, C. F. Johnston, D. V. Sridhara Rao, A. M. Sanchez, and C. J. Humphreys, Appl. Phys. Lett. **93**, 101901 (2008).

[8]B. Lucznik, B. Pastuszka, G. Kamler, I. Grzegory, and S. Porowski, in *Growth of Bulk GaN Crystals by HVPE on Single Crystalline GaN Seeds. Technology of Gallium Nitride Crystal Growth*, edited by D. Ehrentraut, E. Meissner, and M. Boćkowski (Springer-Verlag, Heidelberg, 2010), Chap. 3, pp. 61–78.

[9]H. Teisseyre, C. Skierbiszewski, B. Lucznik, G. Kamler, A. Feduniewicz, T. Suski, P. Perlin, I. Grzegory, and S. Porowski, Appl. Phys. Lett. **86**, 162112 (2005).

[10]B. Heying, X. H. Wu, Y. Li, D. Kapolnek, B. P. Keller, S. P. DenBaars, and J. S. Speck, Appl. Phys. Lett. **68**, 643 (1996).

[11] A. Morel, T. Talierco, P. Lefebvre, M. Gallartz, B. Gil, N. Grandjean, J. Massies, I. Grzegory, and S. Porowski, Mater. Sci. Eng. B **82**, 173 (2001).

[12] F. Natali, Y. Cordier, J. Massies, S. Vezian, B. Damilano, and M. Leroux, Phys. Rev. B **79**, 035328 (2009).

[13] J.-M. Bonard and J.-D. Ganière, J. Appl. Phys. **79**, 6987 (1996).

[14] C. M. Parish and P. E. Russel, Appl. Phys. Lett. **89**, 192108 (2006).

[15] T. Sugahara, H. Sato, M. Hao, Y. Naoi, S. Kurai, S. Tottori, K. Yamashita, K. Nishino, L. T. Romano, and S. Sakai, Jpn. J. Appl. Phys., Part 2 **37**, L398 (1998).

[16] T. Gühne, Z. Bougrioua, P. Vennéguès, and M. Leroux, J. Appl. Phys. **101**, 113101 (2007).

[17] M. A. Moram, C. F. Johnston, M. J. Kappers, and C. J. Humphreys, J. Phys. D: Appl. Phys. **43**, 055303 (2010).

[18] P. Corfdir, J. Ristić, P. Lefebvre, T. Zhu, D. Martin, A. Dussaigne, J.-D. Ganière, N. Grandjean, and B. Deveaud-Plédran, Appl. Phys. Lett. **94**, 201115 (2009).

[19] S. J. Rosner, E. C. Carr, M. J. Ludowise, G. Girolami, and H. I. Erikson, Appl. Phys. Lett. **70**, 420 (1997).

[20] K. Kornitzer, T. Ebner, K. Thonke, R. Sauer, C. Kirchner, V. Schwegler, M. Kamp, M. Leszczynski, I. Grzegory, and S. Porowski, Phys. Rev. B **60**, 1471 (1999).

[21] We consider an absorption coefficient of 10^5 cm^{-1}; See D. Brunner, H. Angerer, E. Bustarret, F. Freudenberg, R. Höpler, R. Dimitrov, O. Ambacher, and M. Stutzmann, J. Appl. Phys. **82**, 5090 (1997).

[22] B. Deveaud, J. Y. Emery, A. Chomette, B. Lambert, and M. Baudet, Appl. Phys. Lett. **45**, 1078 (1984).

[23] M. Leroux, N. Grandjean, M. Laügt, J. Massies, B. Gil, P. Lefebvre, and P. Bigenwald, Phys. Rev. B **58**, R13371 (1998).

[24] A. Dussaigne, P. Corfdir, J. Levrat, T. Zhu, D. Martin, P. Lefebvre, J.-D. Ganière, R. Butté, B. Deveaud-Plédran, N. Grandjean, Y. Arroyo, and P. Stadelmann, Semicond. Sci. Technol. **26**, 025012 (2011).

[25] A. Bellabchara, P. Lefebvre, P. Christol, and H. Mathieu, Phys. Rev. B **50**, 11840 (1994).

[26] N. Akopian, G. Bahir, D. Gershoni, M. D. Craven, J. S. Speck, and S. P. DenBaars, Appl. Phys. Lett. **86**, 202104 (2005).

[27] E. T. Rashba and G. E. Gurgenishvili, Fiz. Tverd. Tela (Leningrad) **4**, 759 (1962) [Sov. Phys. Solid State **4**, 759 (1962)].

[28] D. S. Citrin, Phys. Rev. B **47**, 3832 (1993).

[29] J. Bellessa, V. Voliotis, R. Grousson, X. L. Wang, M. Ogura, and H. Matsuhata, Phys. Rev. B **58**, 9933 (1998).

[30] For (Al,Ga)As/GaAs QWs, see for instance M. Gurioli, J. Martinez-Pastor, M. Colocci, C. Deparis, B. Chastaingt, and J. Massies, Phys. Rev. B **46**, 6922 (1992).

[31] M. Smith, J. Y. Lin, H. X. Jiang, A. Salvador, A. Botchkarev, W. Kim, and H. Morkoç, Appl. Phys. Lett. **69**, 2453 (1996).

[32] L. C. Andreani, F. Tassone, and F. Bassani, Solid State Commun. **77**, 641 (1991); model revised in L. C. Andreani, *Optical Transitions, Excitons, and Polaritons in Bulk and Low-Dimensional Semiconductor Structures. Confined Electrons and Photons: New Physics and Devices,* p. 57, edited by E. Burstein and C. Weisbuch (Plenum, New York, 1995).

[33] For a review, see R. A. Oliver, S. E. Bennett, T. Zhu, D. J. Beesley, M. J. Kappers, D. W. Saxey, A. Cerezo, and C. J. Humphreys, J. Phys. D: Appl. Phys. **43**, 354003 (2010).

[34] I. Vurgaftman, J. R. Meyer, and L. R. Ram-Mohan, J. Appl. Phys. **89**, 5815 (2001).

[35] P. Lefebvre, J. Allègre, B. Gil, A. Kavokine, H. Mathieu, W. Kim, A. Salvador, A. Botchkarev, and H. Morkoç, Phys. Rev. B **57**, R9447 (1998).

[36] B. Deveaud, F. Clérot, N. Roy, K. Satzke, B. Sermage, and D. S. Katzer, Phys. Rev. Lett. **67**, 2355 (1991).

[37] A. Hoffmann, Mater. Sci. Eng. B **43**, 185 (1997).

[38] B. Deveaud, T. C. Damen, J. Shah, and C. W. Tu, Appl. Phys. Lett. **51**, 828 (1987).

[39] L. Lymperakis and J. Neugebauer, Phys. Rev. B **79**, R241308 (2009).

[40] M. Gallart, A. Morel, T. Talierco, P. Lefebvre, B. Gil, J. Allègre, H. Mathieu, N. Grandjean, M. Leroux, and J. Massies, Phys. Status Solidi A **180**, 127 (2000).

[41] S. Krishnamurthy, M. van Schilfgaarde, and N. Newman, Appl. Phys. Lett. **83**, 1761 (2003).

[42] C. Brimont, M. Gallart, A. Gadalla, O. Crégut, B. Hönerlage, and P. Gilliot, J. Appl. Phys. **105**, 023502 (2009).

[43] V. A. Kiselev, B. S. Razbirin, and I. N. Uraltsev, Pis'ma Zh. Eksp. Teor. Fiz. **18**, 504 (1973) [JETP Lett. **18**, 296 (1973)].

[44] H. Tuffigo, R. T. Cox, N. Magnea, Y. Merle d'Aubigné, and A. Million, Phys. Rev. B **37**, 4310 (1988).

[45] A. Tredicucci, Y. Chen, F. Bassani, J. Massies, C. Deparis, and G. Neu, Phys. Rev. B **47**, 10348 (1993).

[46] A. D'Andrea and R. Del Sole, Phys. Rev. B **41**, 1413 (1990).

[47] J. J. Hopfield and D. G. Thomas, Phys. Rev. **132**, 563 (1963).

[48] P. P. Paskov, T. Paskova, P. O. Holtz, and B. Monemar, Phys. Status Solidi A **201**, 678 (2004).

[49] J. J. Hopfield, Phys. Rev. **112**, 1555 (1958).

[50] R. Butté, G. Christmann, E. Feltin, J.-F. Carlin, M. Mosca, M. Ilegems, and N. Grandjean, Phys. Rev. B **73**, 033315 (2006).

[51] P. P. Paskov, B. Monemar, A. Toropov, J. P. Bergman, and A. Usui, Phys. Status Solidi C **4**, 2601 (2007).

[52] G. Neu, M. Teisseire, P. Lemasson, H. Lahreche, N. Grandjean, F. Semond, B. Beaumont, I. Grzegory, S. Porowski, and R. Triboulet Physica B **302-303**, 39 (2001).

[53] M. Leroux, N. Grandjean, B. Beaumont, G. Nataf, F. Semond, J. Massies, and P. Gibart, J. Appl. Phys. **86**, 3721 (1999).

[54] U. Heim and P. Wiesner, Phys. Rev. Lett. **30**, 1205 (1973).

[55] A. K. Viswanath, J. I. Lee, D. Kim, C. R. Lee, and J. Y. Leem, Phys. Rev. B **58**, 16333 (1998).